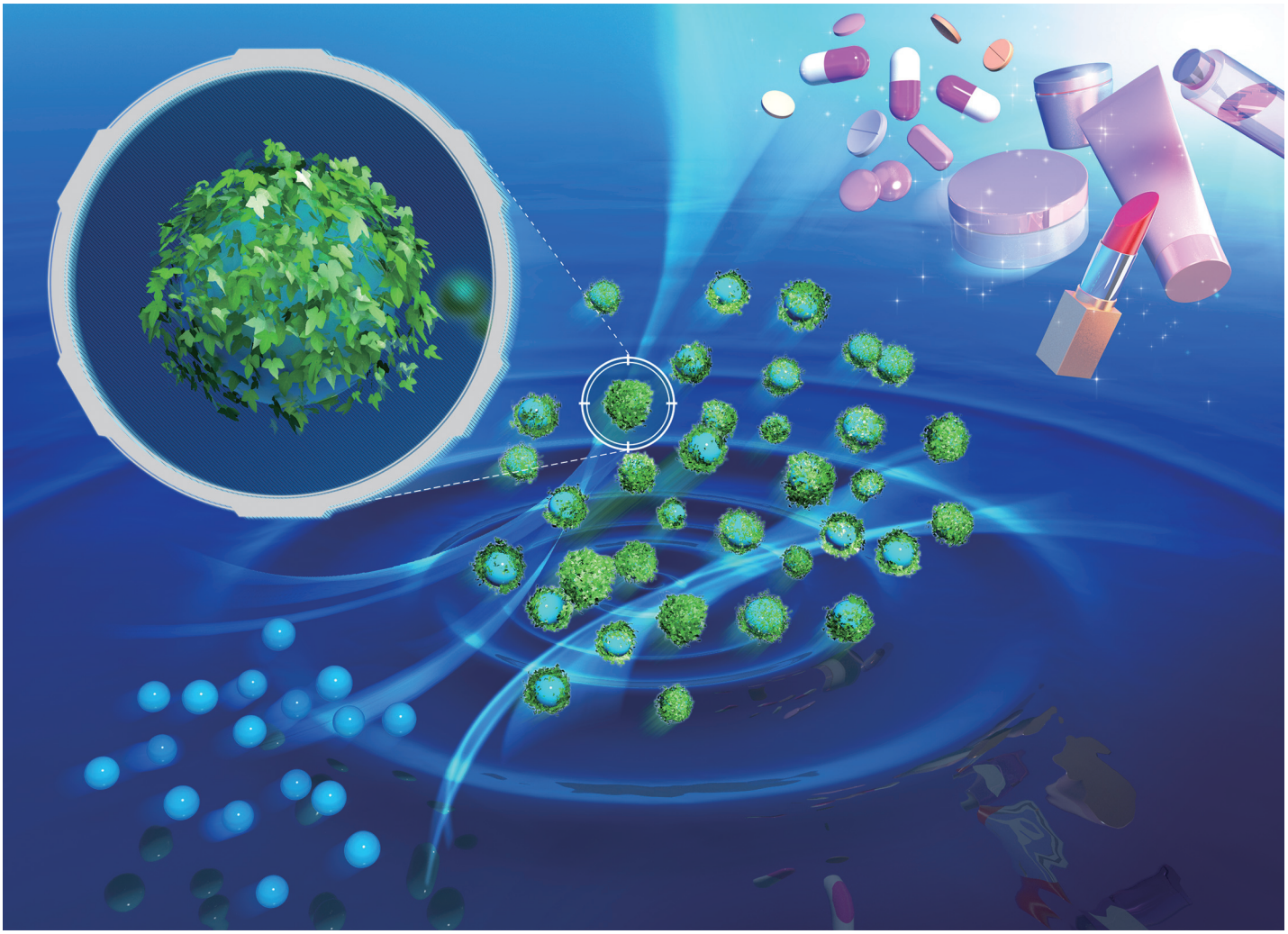

Showcasing research from the Department of Biomaterial Sciences, Graduate School of Agricultural and Life Sciences, The University of Tokyo, Tokyo, Japan.

Fabrication of ultrathin nanocellulose shells on tough microparticles *via* an emulsion-templated colloidal assembly: towards versatile carrier materials

This illustration depicts fabrication of ultrathin layer of plant-based nanomaterial on microcarrier particles. Nanocellulose is a plant-based nanomaterial with unique nanoscale dimension, excellent mechanical properties, and good chemical stability. Ultrathin nanocellulose shells are constructed at the surface of polymer microparticles by emulsion-templated self-assembly. An ~8 nm film nanocellulose film uniformly covers the particles surfaces. The nanocellulose shell renders the microparticles biocompatible and highly dispersible in water. The novel structure offers great potential for future advances in medical and pharmaceutical fields.

As featured in:

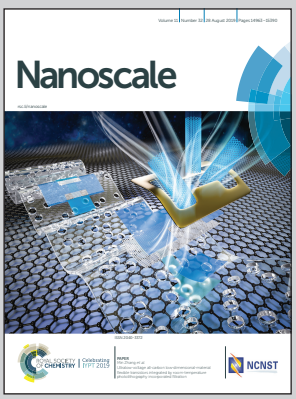

See Shuji Fujisawa *et al.*, *Nanoscale*, 2019, **11**, 15004.

ROYAL SOCIETY OF CHEMISTRY | Celebrating IYPT 2019

rsc.li/nanoscale

Registered charity number: 207890

Nanoscale

COMMUNICATION

View Article Online
View Journal | View Issue

Cite this: *Nanoscale*, 2019, **11**, 15004

Received 26th March 2019,
Accepted 1st June 2019

DOI: 10.1039/c9nr02612f

rsc.li/nanoscale

Fabrication of ultrathin nanocellulose shells on tough microparticles *via* an emulsion-templated colloidal assembly: towards versatile carrier materials†

Shuji Fujisawa, *[a] Eiji Togawa,[b] Katsushi Kuroda,[b] Tsuguyuki Saito [a] and Akira Isogai [a]

Here, we develop a robust approach to forming an ~8 nm thick cellulose nanofiber (CNF) shell on polymer microparticles through an emulsion-templated assembly. The median diameter of the CNF-shelled microparticles was 3.0 μm. The microparticles showed good dispersibility in water with a ζ-potential of −46.7 ± 0.5 mV and had good mechanical resistance. The surface CNF shells showed pH-sensitive drug loading/releasing properties, which suggest potential for a range of therapeutic and biomedical applications.

Engineering assemblies of colloidal nanoparticles is of scientific interest and technologically important for developing new multifunctional surfaces. Various approaches to achieving assemblies have been developed to date, and tailored structures can markedly alter the chemical and physical properties of material surfaces, providing desirable optical, electronic, and catalytic functionalities.[1–3] Templating liquid/liquid interfaces is a robust approach towards self-assemblies of nanoparticles;[4] nanoparticles spontaneously assemble at interfaces, making systems thermodynamically more stable by reducing the interfacial energy.

The interfacial templating strategies offer new opportunities for tailoring the surfaces of micrometre- and submicrometre-sized carrier materials.[5–7] The self-assembly of nanoparticles can be driven at oil/water interfaces of microemulsion systems, or so-called Pickering emulsions. By templating stable Pickering emulsions, nanoparticle-shelled microcarrier particles can be synthesized. An assembled nanocolloidal shell alters the surface and bulk properties of the core material, such as colloidal stability. Furthermore, chemical/biological sensing capabilities are efficiently tuned at their inherently large surfaces. Potential uses of core/shell microcarriers include molecular recognition and drug delivery.[8–10] Inorganic nanoparticles, such as SiO_2 and Fe_3O_4, are typically used as colloidal shells.

Cellulose nanofibers (CNFs) are organic colloidal nanofibrils, and are promising candidates for carrier shells. CNFs can be prepared by refining the hierarchical structure of cellulose in plant cell walls, tunicates, or bacterial cellulose pellicles. This material features unique and well-organized nanostructures, in the range of 2–20 nm in width and several μm in length, depending on the cellulose source.[11–13] Owing to the unique surface characteristics, such as biocompatibility and chemical stability under physiological conditions, CNFs are expected to have applications in biotechnology, including bioscaffolds for cell cultures, efficient drug delivery vehicles, and as agents for immobilization and recognition of enzymes or proteins.[14–16] The drug release properties of CNFs have also been extensively studied in the form of gels, membranes, and coated layers. However, the approach of using CNFs as carrier shells remains unexplored because of the difficulty of constructing well-defined core/shell structures.

Here, we develop an approach to fabricating ultrathin and uniform CNF shell layers on polymer microparticles (Fig. 1a). The well-defined core/shell structure is achieved by an emulsion-templating approach, where the assembly is driven by a decrease in interfacial energy. In this study, CNFs with a width of ~3 nm were prepared from wood cellulose by (2,2,6,6-tetramethylpiperidine-1-oxyl) TEMPO-mediated oxidation.[17] Notably, the TEMPO-oxidized CNF had a high density of carboxy groups on its surface (~1.7 groups per nm^2),[18] which efficiently improved the dispersibility. We investigated the structure and mechanical properties of the CNF-shelled polymer microparticles, and characterized the pH-sensitive affinity of the ultrathin CNF-shell towards therapeutic and biomedical applications.

The ultrathin CNF shell was formed by a spontaneous assembly at the interface of the monomer-in-water Pickering emulsion (Fig. 1a center). The CNF-stabilized Pickering emul-

[a]*Department of Biomaterial Sciences, Graduate School of Agricultural and Life Sciences, The University of Tokyo, Tokyo 113-8657, Japan.*
E-mail: afujisawa@mail.ecc.u-tokyo.ac.jp
[b]*Forestry and Forest Products Research Institute, Tsukuba 305-8687, Japan*

† Electronic supplementary information (ESI) available: Experimental methods, Fig. S1–S3, and Table S1. See DOI: 10.1039/c9nr02612f

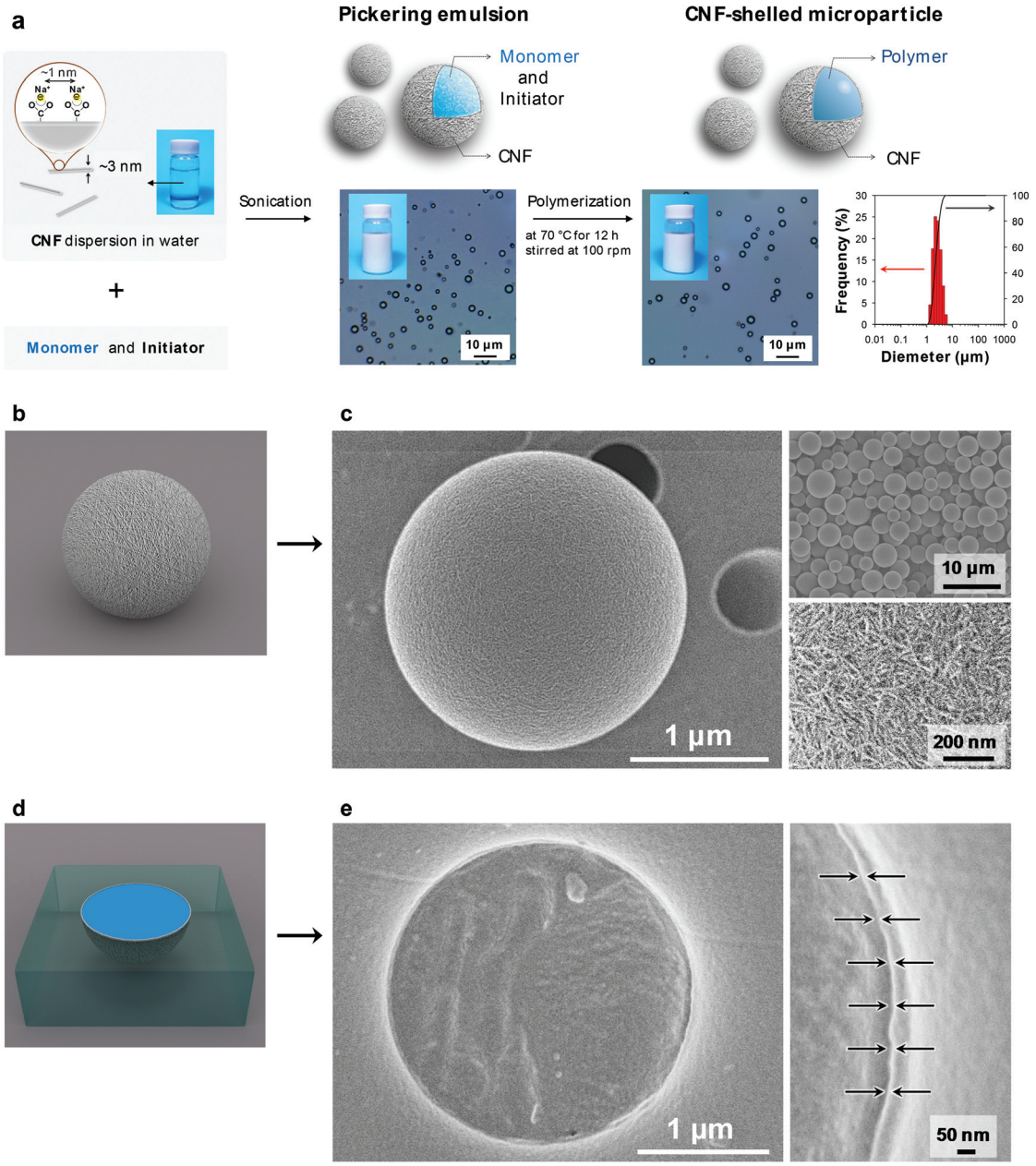

Fig. 1 CNF shell formed on microparticles. (a) Schematic illustration of the synthesis of CNF-shelled microparticles at a 10 : 90 ratio (o/w). CNF-stabilized Pickering monomer-in-water emulsion (center), CNF-shelled microparticle dispersion in water, and size distribution of CNF/polymer microparticles determined by dynamic light scattering analysis showing a median diameter of 3.0 μm (right). (b) Illustration and (c) SEM images of CNF-shelled microparticles (left and top right) and surface (bottom right). (d) Illustration and (e) SEM images of the cross-section of the microparticles embedded in acrylic resin. Black arrows indicate the CNF shell.

sion was prepared by sonicating a mixture of divinylbenzene (DVB) monomer and CNF dispersion in water. The adsorption behaviour of aromatic compounds onto cellulose crystal surfaces has been theoretically and experimentally well-studied. Adsorption takes place at both hydrophilic and hydrophobic crystal surfaces with adsorption energies of the same order of magnitude.[19,20] Therefore, the CNFs favourably attach at the DVB/water interface, driven by an overall decrease in the interfacial energy of the system.[21] The emulsion showed good stability for over a week and no coalescence was observed. The size of the droplets depended on the sonication time. The size decreased with sonication time and the median diameter reached a constant value of ~3 μm, when sonicated for over 1 min (ESI Fig. S2†), which is similar to that of cellulose nanocrystal/styrene emulsions reported by Capron *et al.* (~4 μm).[22]

The CNF-shelled composite microparticles were synthesized by successive polymerization. The microparticles maintained

the size and morphology of the droplets of the original Pickering emulsion even after the polymerization process. The median diameter was 3.0 μm, as determined by dynamic light scattering analysis (Fig. 1a right). The ζ-potential of the microparticle surfaces was −46.7 ± 0.5 mV. These results demonstrate that the microparticles were covered with dense CNF shells. The CNF-shelled microparticles were individually dispersed in water owing to the osmotic pressure arising from the surface anionic charges.

Notably, the size and shape of the original droplets remained intact even after polymerization. Generally, Pickering emulsions show better structural stability than surfactant-stabilized emulsions, because solid particles exhibit better mechanical properties and orders of magnitude higher adsorption energies at oil/water interfaces. By comparison, when water-soluble carboxymethyl cellulose was used as an emulsifier instead of the CNF, the emulsions coalesced during the polymerization (ESI Fig. S3†). Therefore, the CNF provided sufficient mechanical robustness to the emulsions. Furthermore, we confirmed that the uniform size and high surface charges of the CNF in this study played an important role in the synthesis of well-dispersed and uniform composite microparticles (ESI Fig. S3 and Table S1†).

We used scanning electron microscopy (SEM) imaging to visualize the composite structure of the CNF-shelled microparticles (Fig. 1c). The thin shell layer of CNF homogeneously covered the polymer microparticle surfaces (Fig. 1c bottom right, and see ESI Fig. S4†). The inside of the microparticle was filled with polymer, and no voids were observed in the SEM images (Fig. 1e). The thickness of the CNF shell was ~8 nm, calculated based on the weight content of CNFs determined by thermogravimetry-differential thermal analysis (ESI Fig. S5†).

Mechanical properties of individual microparticles were evaluated by micro-compression testing (Fig. 2 and ESI Fig. S6†). The CNF-shelled microparticles exhibited strain at a fracture of 62.3 ± 1.7% and a fracture toughness of 393 ± 29 MJ m^{-3} (Fig. 2b and c). Importantly, there was little effect of the diameter on these values. These results indicate that each microparticle contained a homogeneous and void-free PDVB centre, as confirmed by SEM observations. Moreover, the mechanical properties of these materials were better than those of previously reported styrene–DVB microparticles,[23,24] which we attribute to the denser cross-linked chemical structure formed by DVB. We also examined loading–unloading behaviour (Fig. 2d). Compression and recovery rates varied with the diameter (Fig. 2e and f), because the maximum load was fixed for all samples. The microparticles underwent plastic deformation with a maximum load of 9.8 mN and exhibited slight residual strain after unloading.

Interestingly, with the assistance of the surface carboxy groups of the CNF shell, the microparticle showed a pH-dependent equilibrium adsorption isotherm (Fig. 3b and c). At pH 7.0, the amount of adsorbed methylene blue (MB) at equilibrium (q_{eq}) was higher at all equilibrium concentrations (C_{eq}) compared with that at pH 2.5. This is because the surface carboxy groups are available for ionic bonding with cationic

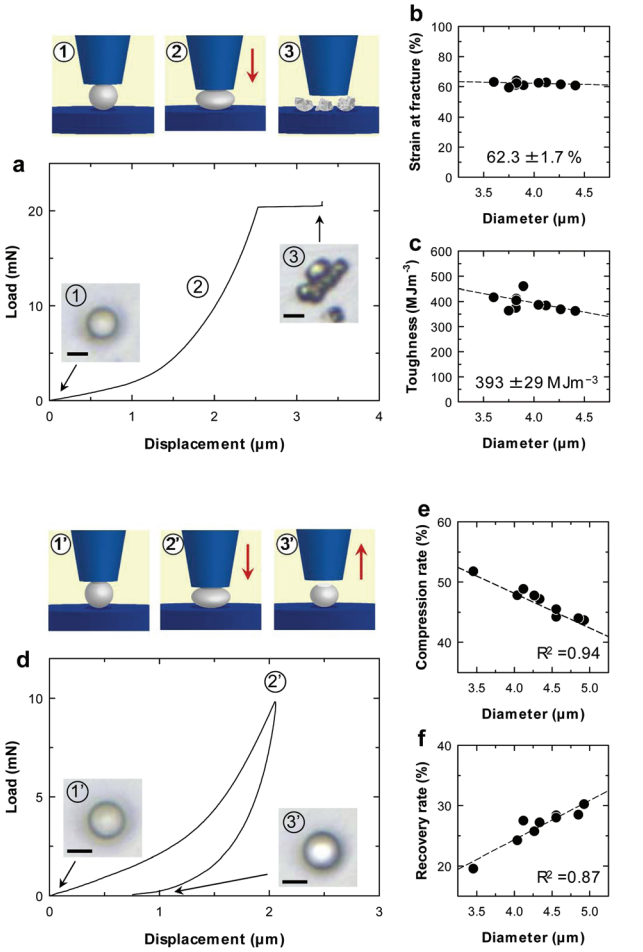

Fig. 2 Mechanical properties of CNF-shelled microparticles. (a) Representative compression curve. Insets show optical microscopy images from the top (scale bars in a and d: 3 μm). (b) Strain at fracture. (c) Fracture toughness. (d) Representative load–unload curve. (e) Compression ratio at maximum load (9.8 mN). (f) Recovery ratio at minimum load.

MB, as is the case for clay minerals.[25] Hence, it is likely that physisorption is the main adsorption mode at pH 2.5 rather than ionic bonding. The equilibrium data at pH 2.5 were fitted with the Langmuir model.[26] At low C_{eq}, the equilibrium data agreed well with the Langmuir model (dotted line in Fig. 3b and c), which is a simple theoretical model for monolayer adsorption with a finite number of adsorption sites. We attribute the steady increase in q_{eq} at higher values of C_{eq} at pH 2.5 for further assembly of MB molecules on the surfaces.[27]

The absorption behaviour was examined by a simple filtration procedure at pH 7.0 (Fig. 3d). The adsorption of MB onto the microparticles was rapid, and the concentration of MB decreased from 5 to 0.06 mg L^{-1} after filtration at a constant flow rate of ~100 mL min^{-1} (Fig. 3e and f). Repeated adsorption/desorption testing was performed by changing the pH in the desorption process (Fig. 3g). After the adsorption of MB at pH 7.0 (cycle 1), the adsorbed MB was washed with an excess of pH 7.0 or 2.5 buffers (cycle 2). Notably, the micropar-

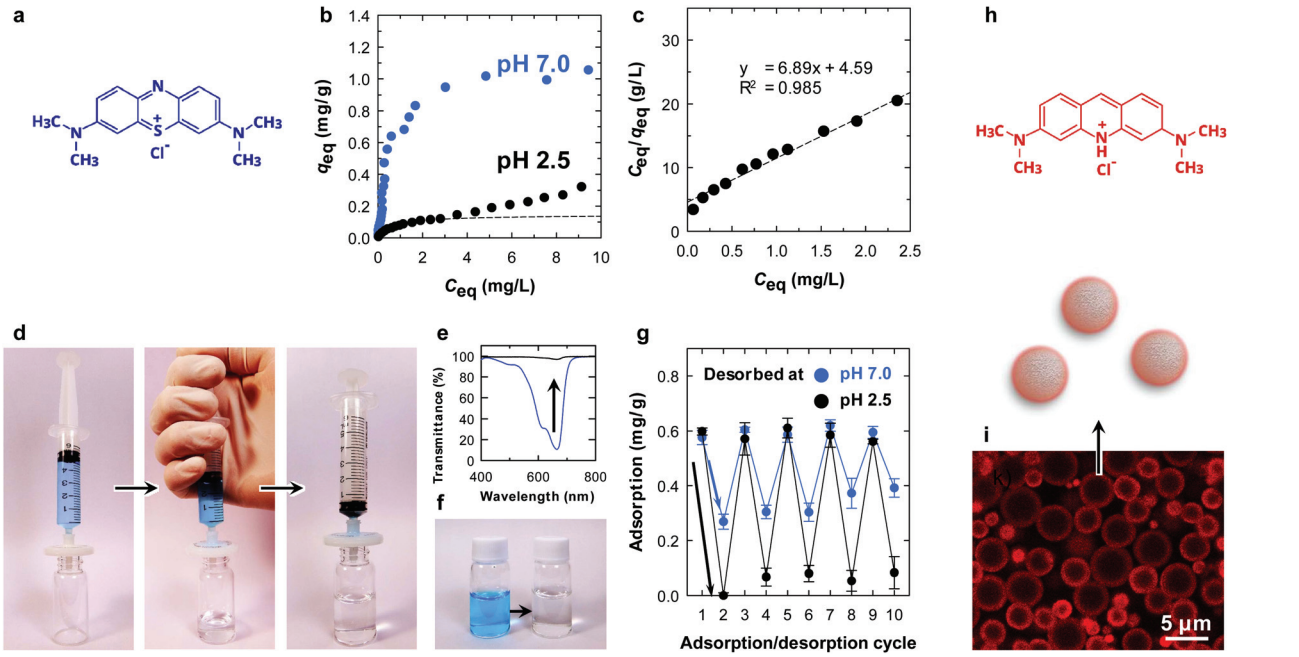

Fig. 3 Adsorption behaviour of MB on CNF-shelled microparticles. (a) Chemical structure of MB; (b) equilibrium adsorption isotherm. (c) Langmuir isotherms of MB onto the microparticles at 23 °C, where dotted lines are obtained by fitting the Langmuir model. (d) Demonstration of MB adsorption before (left), during (center), and after (right) filtration, where 100 mg of CNF-shelled microparticles are retained in the 0.2 μm PTFE membrane filter. (e) Light transmittance spectrum and (f) photograph of the MB solution before and after the filtration. (g) Repeated adsorption/desorption behaviour at pH 7.0 and 2.5, through the filtration. (h) Chemical structure of acridine orange hydrochloride. (i) Confocal laser scanning microscopy image of CNF-shelled microparticles, where surfaces are stained with acridine orange.

ticle showed pH-dependent desorption behaviour. Complete washing at pH 2.5 detached almost all the methylene molecules from the microparticle surfaces. The MB molecules attached through ionic bonding were not released at pH 7.0, as discussed above. MB removal behaviour has been reported so far.[28,29] The adsorption/desorption process was repeatable for at least 10 cycles (Fig. 3g), demonstrating that the core/shell structure is physically stable and the CNFs did not peel from the surfaces during the process. Although the chemical structure of the CNFs on the surfaces was not able to be investigated due to the small amount, the adsorption behaviour was repeatable. This indicates that the CNFs were intact even after the process. The reusability combined with the tough and filterable properties of the microparticles make CNFs have potential applications as column packing materials.

The adsorption behaviour was visualized by confocal laser scanning microscopy, using acridine orange as a fluorescent dye (Fig. 3i). The dye was selectively adsorbed on the surfaces of the microparticles. Notably, the fluorescence of the CNF layers appeared to be thicker than that determined by SEM because the fluorescence image resolution is limited to ~200 nm at a scan depth of ~0.7 μm along the *z* axis.

We examined the pH-sensitive drug release properties of the CNF shell under various pH conditions at 37 °C, using ranitidine and mitomycin C as model drugs (Fig. 4). Ranitidine and mitomycin C are an effective gastric secretory inhibitor and antitumor chemotherapeutic drug, respectively,

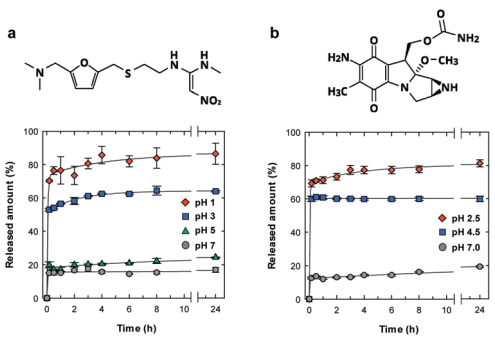

Fig. 4 pH-Responsive drug release behaviour of the CNF-shelled microparticles. (a) Chemical structures and release behaviours of ranitidine, and (b) those of mitomycin C, from the CNF-shelled microparticles under various pH conditions.

and pH-responsive release is needed towards targeted delivery.[30–32] As expected, the microparticles showed preferential drug release under acidic pH conditions, where the drug release was triggered by the dissociation of ionic bonding between anionic CNF and cationic drugs. In acidic solutions of pH of 1 and 2.5 (Fig. 4a and b, respectively), more than 70% of the drug was released within 10 min, which is approximately 4 times as high as the release at pH 7.

The release behaviours by the CNF shells were faster and more pH-selective than those of spray-dried CNF microparti-

cles[33] or CNF-reinforced alginate microspheres,[34] likely because of the good dispersibility and well-defined structure of our microparticles. Generally, CNF gels show slow and sustained drug release properties over a period of several days[35,36] or months,[33,37] because the dense CNF network structure decreases the diffusivity of drug molecules. Although the CNF-shells in this work did not show the slow and long-lasting release properties, this material showed unique pH-triggered release properties and good dispersibility with small sizes. The characteristics of the ultrathin CNF shells are potentially useful for pH-responsive oral and tumour targeted[31,38] drug delivery mediated by nano-/micro-carrier particles.

Conclusions

We prepared the ultrathin CNF shells on microcarrier surfaces, *via* spontaneous CNF assembly at monomer/water interfaces of the emulsion, followed by a polymerization process. The CNF-shelled microparticles exhibited good dispersibility, high toughness, and narrow size distributions, owing to the unique chemical and physical properties of the CNF. The ultrathin CNF shell could be effectively loaded with drug molecules, demonstrating its potential as a pH-sensitive carrier material in adsorption/desorption experiments. Furthermore, the CNF-shelled microparticles could be functionalized by surface modification or encapsulation with other nanomaterials. These unique carrier properties with a versatile range of behaviours show great potential for future advances in medical and pharmaceutical fields.

Conflicts of interest

There are no conflicts to declare.

Acknowledgements

This research was supported by Grants-in-Aid for Scientific Research Grant number JP17K15298 (to S. F.) from the Japan Society for the Promotion of Science (JSPS), and JST-Mirai R&D Program Grant number JPMJMI17ED (to S. F. and T. S.) from the Japan Science and Technology Agency (JST). We acknowledge Miyuki Komura of Olympus Co. Ltd., Japan, for arranging the confocal laser scanning microscopy observation.

References

1 A. N. Shipway, E. Katz and I. Willner, *ChemPhysChem*, 2000, **1**, 18.
2 S. Kinge, M. Crego-Calama and D. N. Reinhoudt, *ChemPhysChem*, 2008, **9**, 20.
3 Y. J. Min, M. Akbulut, K. Kristiansen, Y. Golan and J. Israelachvili, *Nat. Mater.*, 2008, **7**, 527.
4 A. Boker, J. He, T. Emrick and T. P. Russell, *Soft Matter*, 2007, **3**, 1231.
5 S. U. Pickering, *J. Chem. Soc.*, 1907, **91**, 2001.
6 W. Ramsden, *Proc. R. Soc. London*, 1903, **72**, 156.
7 M. P. Zhu, Y. Muhammad, P. Hu, B. F. Wang, Y. Wu, X. D. Sun, Z. F. Tong and Z. X. Zhao, *Appl. Catal., B*, 2018, **232**, 182.
8 F. Q. Tang, L. L. Li and D. Chen, *Adv. Mater.*, 2012, **24**, 1504.
9 Z. W. Niu, J. B. He, T. P. Russell and Q. A. Wang, *Angew. Chem., Int. Ed.*, 2010, **49**, 10052.
10 H. Ma, M. X. Luo, S. Sanyal, K. Rege and L. L. Dai, *Materials*, 2010, **3**, 1186.
11 J. Sugiyama, J. Persson and H. Chanzy, *Macromolecules*, 1991, **24**, 2461.
12 Y. Nishiyama, P. Langan and H. Chanzy, *J. Am. Chem. Soc.*, 2002, **124**, 9074.
13 Y. Nishiyama, J. Sugiyama, H. Chanzy and P. Langan, *J. Am. Chem. Soc.*, 2003, **125**, 14300.
14 N. Lin and A. Dufresne, *Eur. Polym. J.*, 2014, **59**, 302.
15 M. Jorfi and E. J. Foster, *J. Appl. Polym. Sci.*, 2015, **132**, 41719.
16 M. M. Abeer, M. C. I. Mohd Amin and C. Martin, *J. Pharm. Pharmacol.*, 2014, **66**, 1047.
17 A. Isogai, T. Saito and H. Fukuzumi, *Nanoscale*, 2011, **3**, 71.
18 Y. Okita, T. Saito and A. Isogai, *Biomacromolecules*, 2010, **11**, 1696.
19 D. D. Perez, R. Ruggiero, L. C. Morais, A. E. H. Machado and K. Mazeau, *Langmuir*, 2004, **20**, 3151.
20 L. M. Ilharco, A. R. Garcia, J. L. daSilva and L. F. V. Ferreira, *Langmuir*, 1997, **13**, 4126.
21 B. P. Binks and J. H. Clint, *Langmuir*, 2002, **18**, 1270.
22 I. Kalashnikova, H. Bizot, B. Cathala and I. Capron, *Langmuir*, 2011, **27**, 7471.
23 T. Tanaka, T. Suzuki, Y. Saka, P. B. Zetterlund and M. Okubo, *Polymer*, 2007, **48**, 3836.
24 D. O. Kim and J. H. Jin, *J. Appl. Polym. Sci.*, 2007, **104**, 2350.
25 M. Rafatullah, O. Sulaiman, R. Hashim and A. Ahmad, *J. Hazard. Mater.*, 2010, **177**, 70.
26 I. Langmuir, *J. Am. Chem. Soc.*, 1918, **40**, 1361.
27 C. H. Giles, T. H. Macewan, S. N. Nakhwa and D. Smith, *J. Chem. Soc.*, 1960, 3973.
28 H. Liu, D. Q. Yu, T. B. Sun, H. Y. Du, W. T. Jiang, Y. Muhammad and L. Huang, *Appl. Surf. Sci.*, 2019, **473**, 855.
29 P. Hu, Z. X. Zhao, X. D. Sun, Y. Muhammad, J. Li, S. B. Chen, C. J. Pang, T. T. Liao and Z. X. Zhao, *Chem. Eng. J.*, 2019, **356**, 329.
30 M. Kanamala, W. R. Wilson, M. M. Yang, B. D. Palmer and Z. M. Wu, *Biomaterials*, 2016, **85**, 152.
31 S. Ganta, H. Devalapally, A. Shahiwala and M. Amiji, *J. Controlled Release*, 2008, **126**, 187.
32 J. Salonen, L. Laitinen, A. M. Kaukonen, J. Tuura, M. Bjorkqvist, T. Heikkila, K. Vaha-Heikkila, J. Hirvonen and V. P. Lehto, *J. Controlled Release*, 2005, **108**, 362.

33 R. Kolakovic, T. Laaksonen, L. Peltonen, A. Laukkanen and J. Hirvonen, *Int. J. Pharm.*, 2012, **430**, 47.
34 N. Lin, J. Huang, P. R. Chang, L. D. Feng and J. H. Yu, *Colloids Surf., B*, 2011, **85**, 270.
35 H. Paukkonen, M. Kunnari, P. Lauren, T. Hakkarainen, V. V. Auvinen, T. Oksanen, R. Koivuniemi, M. Yliperttula and T. Laaksonen, *Int. J. Pharm.*, 2017, **532**, 269.
36 Y. J. Dong, H. Paukkonen, W. W. Fang, E. Kontturi, T. Laaksonen and P. Laaksonen, *Int. J. Pharm.*, 2018, **548**, 113.
37 R. Kolakovic, L. Peltonen, A. Laukkanen, J. Hirvonen and T. Laaksonen, *Eur. J. Pharm. Biopharm.*, 2012, **82**, 308.
38 E. S. Lee, Z. G. Gao and Y. H. Bae, *J. Controlled Release*, 2008, **132**, 164.